

## Reconstruction of the 3D Geometry of the Ossicular Chain Based on Micro-CT Imaging

MONIKA KWACZ<sup>1,\*</sup>, JAROSŁAW WYSOCKI<sup>2</sup>, PIOTR KRAKOWIAN<sup>3</sup>

<sup>1</sup>*Warsaw Technical University, Faculty of Mechatronics, Warsaw, Poland*

<sup>2</sup>*Institute of Physiology and Pathology of Hearing, Warsaw, Poland*

<sup>3</sup>*Institute of Fundamental Technological Research, Polish Academy of Sciences, Warsaw, Poland*

Modelling of the sound transmission process from the external ear canal through the middle ear structures to the cochlea is often performed using the finite element method. This requires knowledge of the geometry of the object being modelled. The paper shows the results of reconstruction of the 3D geometry of the ossicular chain. The micro-CT images of a cadaver's temporal bone were used to carry out the reconstruction process. The obtained geometry may be used not only for modelling of the middle ear mechanics before and after ossicular replacement but also for production of anatomical middle ear prostheses, calculation of inertial properties of the ossicular bones or educating radiologist and otolaryngologist.

**Key words:** middle ear, micro-CT, 3D geometry

### 1. Introduction

The ossicular chain in the middle ear consists of the malleus, incus and stapes, which transmit acoustic vibrations from the tympanic membrane to fluid vibrations in the cochlea. The middle ear bones are attached to surrounding bony structures by ligaments and tendons and are connected with each other by two joints. The middle ear components have a miniature and complex geometry, and play a crucial role in sound transmission. Sound waves collected and conveyed by the external ear canal are first transformed into mechanical vibrations of the tympanic membrane and the ossicular chain, and then transformed into travelling waves in the fluid-filled cochlea (inner ear).

Degradation of the ossicles through chronic inflammatory processes leads to hearing loss and requires a surgical reconstruction, often using a middle ear ossicular

---

\* Correspondence to: Monika Kwacz, Warsaw Technical University, Faculty of Mechatronics, 02-525 Warsaw, ul. św. A. Boboli 8, e-mail: m.kwacz@mchtr.pw.edu.pl  
*Received 03 March 2011; accepted 07 July 2011*

prosthesis. Sometimes, especially in otosclerosis treatment, a special stapes prosthesis is needed. Many different types of prostheses are now used depending on the ear pathology occurring and preference of the surgeon [1, 2]. Advances in otology and bioengineering led to new surgical reconstruction techniques and implantable hearing devices. Devices for hearing restoration to middle ear conductive impairments are often mechanical by nature and thus can be studied using mechanical or analogue computational models. A recent computational model has been used to simulate the behaviour of the middle ear in order to understand relationship between its structure and function. Such an understanding could help to improve the design and function of prosthetics and to improve methodologies and planning of surgical procedures in the middle ear. To formulate an accurate biomechanical model, individual anatomy may be important, which requires a fast and non-destructive method.

Finite element method (FEM) is a powerful and flexible computer-based approach to create 3D models of the middle and inner ear, for the purposes of both simulation and evaluation of effectiveness of various types of the ossicular prosthesis [3, 4]. The model can be used to simulate the detailed vibration modes, stress distributions and dynamic behaviour at any location in the hearing organ [5, 6]. Funnell and Laszlo (1978) [7] first published a finite-element model of the cat eardrum. Since then a number of groups have used the FEM to study the mechanics of the vibration of the tympanic membrane and the ossicular chain in humans [6, 8–12].

The finite element method requires knowledge of the geometrical and material parameters of the analysed structures. To obtain three-dimensional anatomical information about the ossicular chain, traditional histological methods can be used, however, they are destructive and require several months for results to be obtained. Investigations into reconstruction of the middle ear geometry have been reported in several papers [9, 13–17]. Funnell et al. [13] first used histological sections of the cat middle ear to reconstruct the geometry of the ossicles, the posterior incudal ligament and the manubrium for the finite element (FE) model.

The morphology of the middle ear is very complicated; therefore recently the most common method is the micro-scale X-ray computed tomography imaging. X-ray microtomography (micro-CT) is a new technique allowing visualization of the internal structure with a quasi-histological quality. Detailed 3D reconstruction of the ear structures requires both thin sections and high spatial resolution. Therefore micro-CT is a useful method for imaging and diagnosis of the middle and inner ear. This technique appears to be ideally suited for obtaining the realistic anatomical geometries to be used with physics-based modelling to simulate the middle ear, instead of fitting of model parameters to measurements from average ears. The first application of the micro-CT to obtain general geometry of the middle ear bones was found to have more clarity than obtained with MRI [18–20].

This paper presents the results of the first in Poland application of the micro-CT for visualization of the middle ear structure in human temporal bones and for determining of the three-dimensional (3D) geometry of the ossicular chain. The obtained

geometry will be used for the finite element modelling of the middle ear mechanics before and after the stapedotomy surgery with a new stapes prosthesis.

## 2. Methods

The geometrical 3D model of the ossicular chain was obtained from a 3D reconstruction from micro-CT images of the left cadaveric temporal bone. The method we used consisted of three stages: (1) the human cadaver's temporal bone preparation, (2) the micro-CT scanning process and the image acquisition, (3) the image processing and 3D reconstruction.

### 2.1. Human Temporal Bone Preparation

#### 2.1.1. Temporal Bone Preparation

The human cadaver's temporal bone was dissected at the Forensic Medicine Department, Warsaw Medical University, during a routine autopsy from a 47 years old male cadaver. The temporal bone was harvested within 2 days of death and frozen immediately upon extraction. The dissection was performed in the Clinical Anatomy Laboratory of the Head and Neck, International Center of Hearing and Speech, Kajetany, Poland. Soft tissues were removed from the specimen using a set of standard surgical tools. Under microscopic visualization simple mastoidectomy and hypotympanotomy were performed and the external auditory meatus and the middle ear cavity were visualised widely to minimize X-ray attenuation and to reduce the specimen size so as to allow increasing of the scan resolution. On the basis of topographical landmarks such as: pyramidal apex, mastoid process, stylomastoid process/foramen and internal as well as external auditory meatus, the bone was oriented and fixed in plastic box.

### 2.2. Micro-CT Scanning Process and the Image Acquisition

#### 2.2.1. Micro-CT System

In this study a micro-CT system "SkyScan 1076" developed by Skyscan (Kontich, Belgium, [www.skyscan.be](http://www.skyscan.be)) was used to obtain high resolution scans of the fresh human cadaver's temporal bone (Fig. 1). The system allows acquiring of three-dimensional images of the test object without its destruction. 3D image is created as a result of the reconstruction process performed from a series of two-dimensional X-ray images. The micro-CT system consists of the X-ray lamp with a high voltage power supply, one bed for the sample with a precise object positioning mechanism and a CCD camera connected to a computer with software for storing and processing of the received data. The X-ray tube is in the range from 20 kV to 100 kV with a maximum power of 10W and can reach a spot diameter of 5 micrometers. The data

are obtained by rotating the X-ray tube and the CCD cameras for up to 180 degrees or 360 degrees, with adjustable increments (at least 0.02 degree) around the axis of the immovable object. The resulting images are saved as 16-bit TIFF files. Reconstruction of the object is carried out “off-line” after the end of the data collection (two-dimensional X-rays). Feldcampus modified algorithm is used to create a set of cross sections and then to obtain a realistic 3D model with the possibility to rotate and cut it at any angle. The obtained 3D model can be saved in STL, P3G or CTM format and then imported into specialized software for further processing.

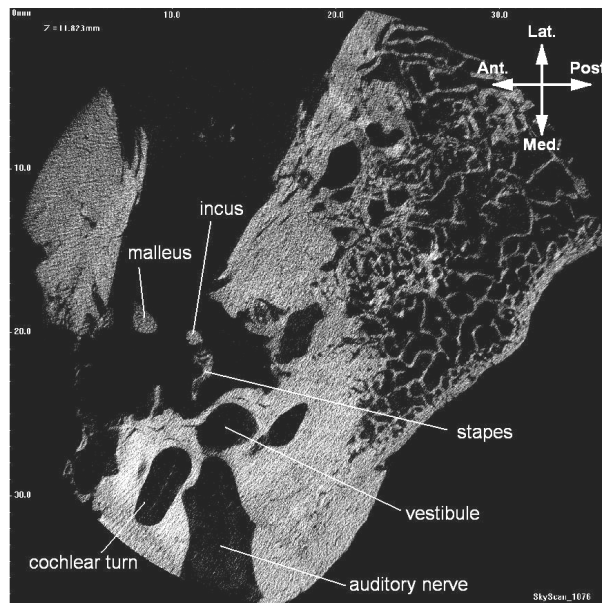


**Fig. 1.** One micro-CT image of an intact left ear from a human cadaver’s temporal bone preparation obtained from SkyScan 1076 micro-CT System with 18.0  $\mu\text{m}$  resolution

### 2.2.2. Parameters of the Scanning Process

The specimen was placed on a rotation plate and radio-graphed during a step-by-step 360deg rotation. The scanning resolution in this study was 18  $\mu\text{m}$ . The scans were performed with a source voltage and source current of, respectively, 100 kV and 100  $\mu\text{A}$ . The maximum X-ray intensity setting of 100  $\mu\text{A}$  was used to get sufficiently good signal-to-noise ratio and good image clarity. An aluminium filter with a thickness of 1mm was used to narrow the X-ray energy spectrum, reducing the low energy component, thus reducing beam hardening. The scanning exposure time per frame was 220 ms. The images were acquired at a step angle of 0.7° for a total circular orbit of 360°. The cone beam acquisitions save all of the projection images as 16-bit TIFF files. In order to improve quality of the final image file, averaging of five images was conducted. Following the acquisition, an axial slice-by-slice reconstruction was performed.

### 2.2.3. Reconstruction

The SkyScan's volumetric reconstruction software "NRecon 1.5.1.1." was used to create a set of cross section slices through the object. The final projection images in 16-bit TIFF format were input into the "NRecon" software and then the following parameters of the reconstruction process were defined: Smoothing=1, Ring Artifact Correction=10, Undersampling Factor=1, Threshold for defect pixel mask (%)=0, Beam Hardening Correction (%)=17. The output files were saved in 8-bit grayscale BMP format at the resolution 2000 x 2000 pixels. Figure 1 shows an example of one slice images of the intact left ear. The stack of the slice images (460 BMP images) was then used for segmentation and 3D volume reconstruction of the ossicular chain.

## 2.3. Image Processing, Three-dimensional Reconstruction and Mesh Generation

The ScanIP/ScanFE™ software (Simpleware Ltd, UK, [www.simpleware.com](http://www.simpleware.com)) was used for the image processing, the three-dimensional geometry reconstruction and the mesh generation. ScanIP image processing software provides an extensive selection of image processing tools to assist the user in visualising and segmenting the regions of interest from any volumetric 3D data (e.g. MRI, CT, micro-CT) [21]. The software package offers a range of segmentation and visualisation tools that enable to create any number of masks (parts). The segmentation tools include thresholding, region growing, Boolean and morphological operations, flood fill, point edit, overlap check, noise reduction filters, etc. On our development computer, containing a quad-core Intel Core i7 Q 820 processor (Intel, Santa Clara, CA) with an NVIDIA GeForce GT 320M (NVIDIA, Santa Clara, CA) video card with 1024 MB memory, the ScanIP/ScanFE software is fully interactive at full screen resolution, running with high rendering quality. Often the limiting factor is video card speed, particularly the number and speed of its shading units.

A stack of the slice images (460 BMP images) was processed by the ScanIP program, and then the cropping, filtering and segmentation of the interesting structures was carried out.

### 2.3.1. Cropping

The data originally contained more space than the specimen actually occupied. A cropping was therefore performed in order to preserve only the extents of the data containing the specimen. This resulted in a smaller volume, close tight to the data.

### 2.3.2. Filtering

Due to the noisy nature of the image, some filtering was necessary. The Curvature Anisotropic Diffusion filter, offered by ScanIP was therefore used. It should be noted that it is considered more as a Noise Reduction filter, rather than a Smoothing Filter. The reason

is that its purpose is to reduce noise while preserving features, which is not the case in smoothing filters such as Gaussian filtering. The Curvature Anisotropic Diffusion filter was applied with a conductance of 5, a time step of 0.0625, and 10 iterations.

### 2.3.3. Segmentation

Segmentation is an image processing technique that partitions an image into meaningful regions or structures of interest. The goal of segmentation is to separate the image points representing a particular object from the rest of the image.

The first step was a separation of the stapes from an oval window niche. Because the grayscale differences between stapes and annular ligaments in the oval window were too small, the automatic contouring couldn't be used, and manual segmentation was required. Due to the noisy nature of the image, some filtering was necessary. The Morphological and Smoothing filters were therefore used. Then, one segmentation mask representing the whole ossicular chain was generated from pixels of values ranging from 2 to 255. The reconstructed 3D geometry of the ossicular chain is shown in Fig. 2.

The second step was a manual separation of the ossicular bones both in the incus-malleus joint and in the incus-stapes joint. After the segmentation, three masks were created using ScanIP: (1) Malleus, (2) Incus and (3) Stapes. The segmented images were exported as STL files or, after the meshing procedure with the ScanFE module, exported directly to leading commercial finite element packages.

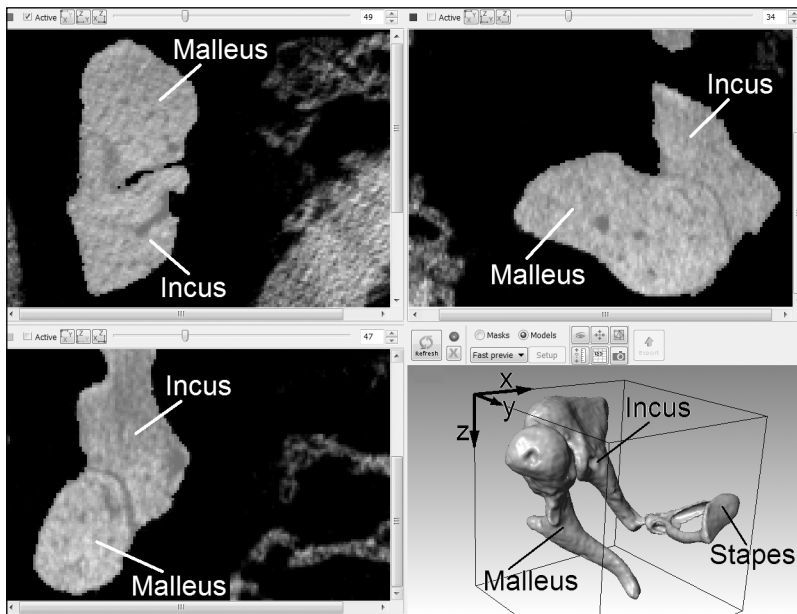
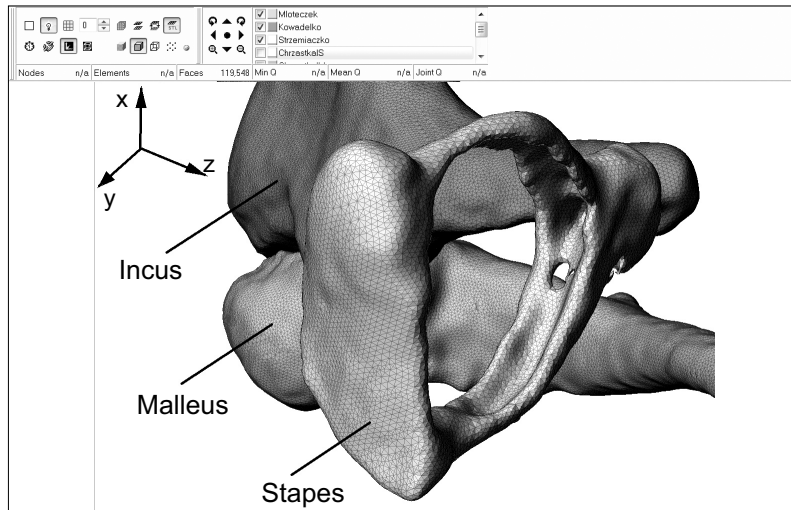


Fig. 2. The incus-malleus joint before segmentation and the reconstructed 3D geometry of the ossicular chain (ScanIP)

### 2.3.4. Meshing

The ScanFE software was thereafter used to generate a number of the finite element meshes based on the 3D segmented image data. The meshing software tool automatically generates the mesh from the parts (masks) created by ScanIP (Fig. 3).



**Fig. 3.** Volumetric mesh of the reconstructed 3D geometry (+ScanFE)

The approach used is based on post-processing a ‘voxel’ based mesh using techniques adapted from image processing to provide volumetric meshes with smooth outer boundaries for the different parts as well as smooth interfaces between parts. The meshing approach also incorporates an adaptive meshing scheme, which significantly reduces the degrees of freedom of the mesh [22].

Based on the three segmented structures (malleus, incus and stapes), two smooth models of different mesh densities were generated using +ScanFE taking less than 4 minutes each. To generate the smooth mesh the following Mesh options were applied: Mesh type smoothed, Minimum quality target of 0.15, Max curvature of 0.5 and Max iterations 2. Then, material properties were assigned via mapping from the grey scale in the underlying CT data using the relationships shown in the Table 1.

**Table 1.** Material properties based on functions of the greyscale [23]

Material properties	Relationship
Mass density ( $\rho$ )	$\rho = 1000 + 0.54559 \cdot GS$
Young’s Modulus ( $E$ )	$E = 0.4249 \cdot \rho^3$
Poisson’s ratio ( $\mu$ )	$\mu = 0.3$

where  $GS$  stands for the grayscale value in Hounsfield units HU

After meshing and configuring the material properties the contact surfaces were defined and then nodes, elements, material properties, contact surfaces of the whole ossicular chain were exported to input format files for the ANSYS package.

### 3. Results

#### 3.1. Three-dimensional Visualization

We used the ScanIP™ software (Simpleware Ltd, Exter, UK) to examine micro-CT scans of human temporal bone. The dataset was prepared by cropping and down-scaling as previously described. Figure 4 demonstrate the visual results of volume rendering based on high-resolution micro-CT datasets. The general statistical information on the image data and parameters of the volume models of the malleus, incus and stapes are shown in the Table 2.

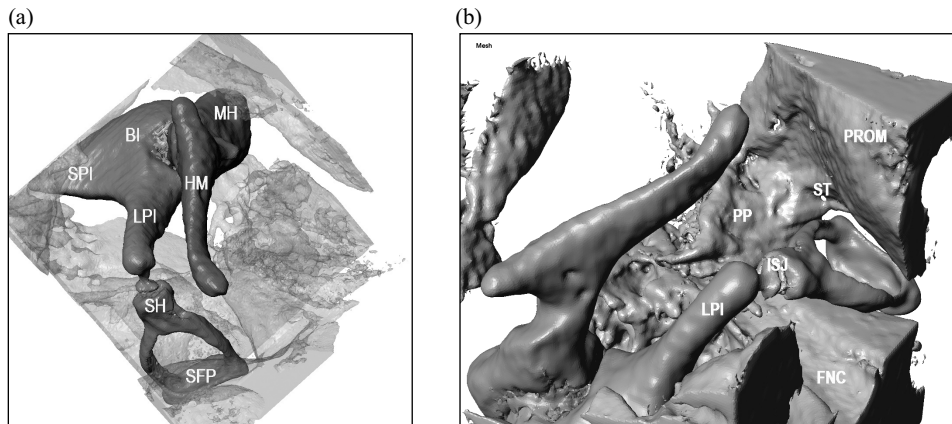


**Fig. 4.** Rendering of the ossicles and the middle ear landmarks using the volume renderer. (a) The body of the incus (BI), handle of the malleus (HM), long process of the incus (LPI), malleus head (MH), stapes footplate (SFP), stapes head (SH), short process of the incus (SPI). (b) facial nerve canal (FNC), incudo-stapedial joint (ISJ), sinus tympani (ST), pyramidal process (PP), and promontory (PROM) are shown

**Table 2.** General statistical information on the image data and parameters of the volume models of the malleus, incus and stapes

	Malleus	Incus	Stapes	Ossicular Chain
Voxels	113 929	144 301	14 840	277 739
Volume [mm <sup>3</sup> ]	14.2	18.0	1.86	34.7
Face Area [mm <sup>2</sup> ]	70.9	77.9	32.5	173.0
Est. hex/tet elements	286 036	335 206	83 525	693 567
Est. all tet elements	643 654	794 672	100 617	1 554 643
Mean G.S.	75.8	105.0	61.4	89.6
Std.Dev.G.S.	37.0	42.5	42.5	43.5

In the Table 2 each row contains:

**Voxels:** the number of voxels contained within the mask (malleus: 113929, incus: 144301, stapes: 14840, and the whole ossicular chain: 277739 voxels).

**Volume [mm<sup>3</sup>]:** the total mask volume, treating each voxel within the mask as a cuboid (malleus: 14.2 mm<sup>3</sup>, incus: 18.0 mm<sup>3</sup>, stapes: 1.86 mm<sup>3</sup>, and the whole ossicular chain: 34.7 mm<sup>3</sup>).

**Face Area [mm<sup>2</sup>]:** the total external face area, including faces that adjoin the edge of the domain (malleus: 70.9 mm<sup>2</sup>, incus: 77.9 mm<sup>2</sup>, stapes: 32.5 mm<sup>2</sup>, and the whole ossicular chain: 173.0 mm<sup>2</sup>).

**Est. hex/tet elements:** an estimate of the total number of volumetric elements that would be present if the mask is used to form a mesh from a mixture of hexahedral and tetrahedral elements. This value should only be used as a guide, and is usually accurate to within  $\pm 10\%$ . The estimate does not take into account any interior mesh adaptation, which can significantly reduce the number of elements in the final mesh.

**Est. all tet elements:** an estimate of the total number of volumetric elements that would be present if the mask is used to form a mesh from only tetrahedral elements.

**Mean G.S.:** the mean greyscale value for voxels.

**Std.Dev.G.S.:** the standard deviation of the greyscale value for voxels.

The results of the some morphometric measurements of the ossicles are shown in Fig. 5.

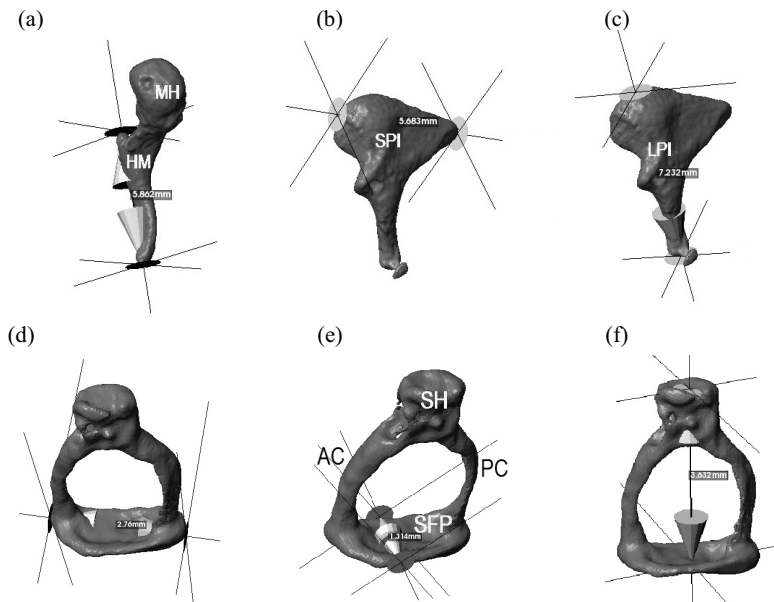


**Fig. 5.** Morphometric measurements of the malleus, the incus and the stapes: (a) length of the handle of the malleus (HM) – 5.9 mm, (b) length of the short process of the incus (SPI) – 5.7 mm, (c) length of the long process of the incus (LPI) – 7.2 mm, (d) maximal length of the stapes footplate – 2.8 mm, (e) width of the stapes footplate – 1.3 mm, (f) total height of the stapes – 3.6 mm

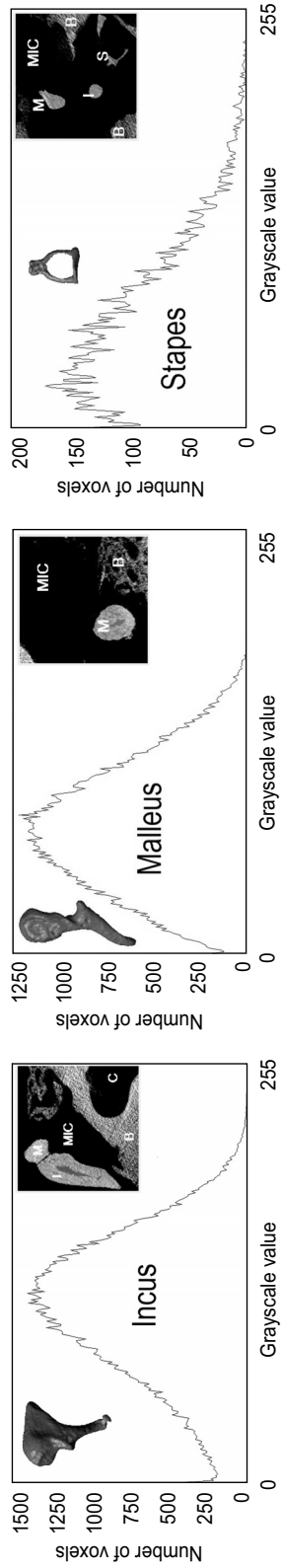


**Fig. 6.** Histograms of the grayscale value of the malleus, the incus and the stapes based on masks. On slice images: M – malleus, I – incus, S – stapes, B – surrounding bone structures, and C – cochlea filled with fluid

Figure 6 shows the histograms of the greyscale value of the malleus, the incus and the stapes based on their masks.

Portions of the malleus and incus bones are vascularised and thus contain lower density blood vessels. Due to high resolution of the scanning process it is possible to see partially the internal microscopic channels (blood vessels, lymphatic channels) and the centrally located marrow spaces of the incus (Fig. 7a) and malleus (Fig. 7b) on the slice images and thus to estimate their volume over the total ossicle volume. The greyscale values for the bone have a higher range (100–200 GS) than for blood vessels (50–100 GS) and air (below 50). Consequently, the entire bone cannot be treated with uniform density. No internal cavities were found in the stapes.

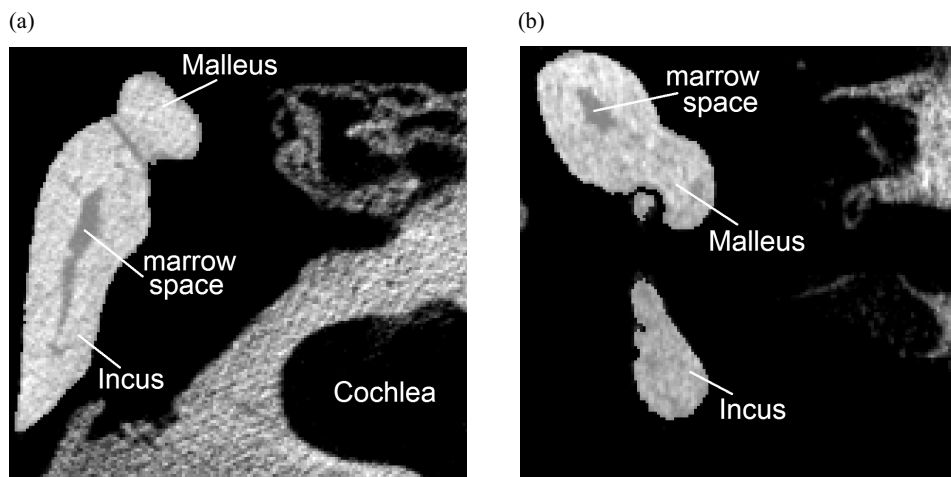


**Fig. 7.** The internal microscopic channels of the (a) incus and (b) malleus. These bones contain “high density” bony parts and “low density” parts consisting of blood vessels and lymphatic channels

### 3.2. Meshing for Finite Element Modeling

We used the ScanFE<sup>TM</sup> software (Simpleware Ltd, Exter, UK) to generate finite element mesh, define greyscale-derived material properties and export the volume mesh as Finite Element Model. The software generates an initial mesh consisting only of voxel elements in which the surfaces of parts are inherently unsmoothed. The meshing procedure provides the controls for generating a high-quality smoothed surface mesh on the exterior of each part and for adapting the non-surface interior mesh of parts. The resulting mesh consists of a mixture of tetrahedral and hexahedral elements. Internal voxels was converted to hexahedral elements and the surface voxels to tetrahedral elements. Table 3 shows a mixed hexahedral and tetrahedral element volumetric mesh obtained from the reconstructed 3D geometry of the ossicular chain. The mesh consists of either linear or quadratic (mid-side noded) elements. In our study the ossicular chain consists of 206 549 nodes, 738 793 elements,

113 771 hexahedral elements and 625 022 tetrahedral elements, the malleus consists of 83 687 nodes, 49 018 hexahedral elements and 253 824 tetrahedral elements, the incus consists of 95 578 nodes, 57 933 hexahedral elements and 291 373 tetrahedral elements, and the stapes consist of 27 263 elements, 6 820 hexahedral elements, and 79 801 tetrahedral elements.

**Table 3.** Mixed hexahedral and tetrahedral element volumetric mesh of the ossicular chain. In the table number of nodes, total elements, hexahedral elements, and tetrahedral elements of the malleus, incus, stapes, and ossicular chain are shown

	Malleus	Incus	Stapes	Ossicular Chain
Nodes	83 687	95 578	27 263	206 549
Elements	302 842	349 306	86 621	738 793
Hex. Elements	49 018	57 933	6 820	113 771
Tet. Elements	253 824	291 373	79 801	625 022

Material properties (Mass Density, Young's Modulus and Poisson's Ratio) within each of elements of the ossicular chain were assigned on the basis of functions of the greyscale value of the original data. The relationships between the greyscale value in the scanned data and the physical properties of the cortical bone are shown in Table 1. The volume mesh with the material properties can be directly imported into e.g. ANSYS package.

#### 4. Discussion

This study demonstrates that micro-CT and 3D reconstruction of the ossicular chain is technically feasible and gives a view of the anatomy that correlates well with that obtained using traditional histology. We have developed a 3D virtual ossicular chain model based on the micro-CT imaging of the cadaver temporal bone specimens. However, in addition to simply depicting anatomy, the information obtained can be integrated into a finite element model. The quantitative measurements of the 3D geometry of the middle ear structures are very important for proper modelling of sound conduction.

Micro computed tomography provides high resolution 3D volumetric data suitable for analysis, quantification, validation and visualization of the results. The micro-CT presents unique opportunities for highly quantitative three dimensional imaging of cadaver's temporal bone preparations both in physiological and implanted state. It is a structural imaging modality that can differentiate contrast-enhanced tissues or structures with a high attenuation factors from non-enhanced soft tissues. Traditional use of the micro-CT includes in vivo and in vitro imaging applications such as screening for anatomical abnormalities and detection and quantification of anatomical changes in hearing organ. The spatial resolution of micro-CT volumes

depends strictly on the X-ray source/detector geometry, which depends on the type of scanner. Data from three dimensional imaging modalities consist of a regular Cartesian grid of greyscale data representing the relative signal strength throughout the scanned volume obtained from the imaging modality.

Although processing of the micro-CT images is very complicated, the micro-CT technique is currently the best tool that allows to obtain the morphometry of a cadaver's temporal bone specimens at a very high resolution. 3D visualisation allows easy understanding of the anatomy and pathology of the human hearing organ and may support patient and student education in the field of otology and audiology.

## 5. Conclusions

The objective of this study was to develop a semi-automatic method for creation of the 3D models of the ossicular chain on the basis of micro-CT data.

The resulting morphometry data are important for anatomically based 3D computational models of the process of sound transmission from the external ear canal through the middle ear structures to the cochlea. The obtained geometry may be used not only for modelling of the middle ear mechanics (e.g. before and after the ossicular replacement) but also for production of anatomical middle ear prostheses, calculation of inertial properties of the ossicular bones or educating radiologists and otolaryngologists.

We are currently working on building an finite element model of the middle ear mechanics and the obtained 3D geometry will be used for this modelling before and after stapedotomy surgery with a new stapes prosthesis.

## Acknowledgments

We gratefully acknowledge the Institute of Physiology and Pathology of Hearing for kindly providing the temporal bone and the Medical University of Warsaw for rendering available the micro-CT.

## References

1. Jahnke K.: *Middle Ear Surgery*, Thieme, Stuttgart – New York 2004.
2. Neudert M., et al.: Partial Ossicular Reconstruction: Comparison of Three Different Prostheses in Clinical and Experimental Studies. *Otol. Neurotol.* 2009, 30 (3), 332–338.
3. Ferris P., Prendergast P.: Middle ear dynamics before and after ossicular replacement. *Journal of Biomechanics* 2000, 33, 581–590.
4. Kelly D., Prendergast P., Blayney A.: The Effect of Prosthesis Design on Vibration of the Reconstructed Ossicular chain: A Comparative Finite Element Analysis of Four Prostheses. *Otol. Neurotol.* 2003, 24, 11–19.
5. Gan R., Sun Q., Dyer R., Chang K., Dormer K.: Three-dimensional Modeling of Middle Ear Biomechanics and its Applications. *Otol. Neurotol.* 2002, 23, 271–280.

6. Koike T., Wada H., Kobayashi T.: Modeling of the human middle ear using the finite-element method. *J. Acoust. Soc. Am.* 2002, 111 (3), 1306–1317.
7. Funnell W., Laszlo C.: Modelling of the cat eardrum as a thin shell using the finite-element method. *J. Acoust. Soc. Am.* 1978, 63 (5), 1461–1467.
8. Wada H., Metoki T., Kobayashi T.: Analysis of dynamic behavior of human Middle ear Using a finite-element method. *J. Acoust. Soc. Am.* 1992, 92 (6), 3157–3168.
9. Beer H., et al.: Modeling of components of the human middle ear and simulation of their dynamic behaviour. *Audiol. Neuro-Otol.* 1999, 4, 156–162.
10. Bornitz M., et al.: Identification of parameters for the middle ear model. *Audiol. Neurotol.* 1999, 4, 163–169.
11. Prendergast P., et al.: Vibroacoustic modeling of the outer and middle ear using the finite-element method. *Audiol. Neurotol.* 1999, 4, 185–191.
12. Sun Q., Gan R., Chang K., Dormer K.: Computer-integrated finite element modeling of human middle ear. *Biomech. Model. Mechanobiol.* 2002, 1 (2), 109–122.
13. Funnell W., Khanna S., Decraemer W.: On the degree of rigidity of the manubrium in a finite element model of the cat eardrum. *J. Acoust. Soc. Am.* 1992, 91(4), 2082–2090.
14. Takagi A., Sando I.: Computer-aided three-dimensional reconstruction: a method of measuring temporal bone structures including the length of the cochlea. *Ann. Otol. Rhinol. Laryngol.* 1989, 98, 515–522.
15. Fujiyoshi T., Mogi G., Watanabe T., Matsushita F.: Undecalcified temporal bone morphology: a methodology useful for gross to fine observation and three-dimensional reconstruction. *Acta Otolaryngol. (Stockholm)* 1992, (Suppl 493), 7–13.
16. Beer H., Bornitz M., Drescher J., Schmidt R., Hardtke H.: Finite element modeling of the human eardrum and applications, In: K. Huttenbrink (ed.), *Middle ear mechanics in research and otosurgery*, Dresden University of Technology, Dresden 1996, 40–47.
17. Weistenhöfer C., Hudde H.: Determination of the shape and inertia properties of human auditory ossicles. *Audiol. Neuro-Otol.* 1999, 4, 192–196.
18. Decraemer W., Dircks J., Funnell W.: Three-Dimensional Modelling of the Middle-Ear Ossicular Chain Using a Commercial High-Resolution X-Ray CT Scanner. *JARO* 2003, 4, 250–263.
19. Lane J., et al.: Imaging microscopy of the middle and inner ear: Part I: CT microscopy. *Clinical Anatomy* 2004, 17 (8), 607–612.
20. Lane J., et al.: Imaging microscopy of the middle and inner ear: Part II: MR microscopy. *Clinical Anatomy* 2005, 18 (6), 409–415.
21. Johnson E.: From 3D Image to Mesh, *The Focus* 2005, 39, 2–5.
22. Weber I., Young P.: Automating the generation of 3D finite element models based on medical imaging data: application to head impact. Simpleware Ltd/University of Exeter, <http://www.simpleware.com/resources/files/3dmodelling.pdf> (Accessed 2011. May.30)
23. Carter D., Hayes W.: The compressive behaviour of bone as a two phase porous structure. *J. Bone Joint Surg.* 1997, 59, 954–962.